

# Mathematical Modeling of CO<sub>2</sub>/CH<sub>4</sub> Separation by Hollow Fiber Membrane Module Using Finite Difference Method

Ahmad Arabi Shamsabadi<sup>1</sup>, Ali Kargari<sup>2,\*</sup>, Foroogh Farshadpour<sup>2</sup> and Saeed Laki<sup>2</sup>

<sup>1</sup>*Petroleum University of Technology, Koot Abdullah, Ahwaz, Iran*

<sup>2</sup>*Membrane Processes Research Laboratory (MPRL), Department of Petrochemical Engineering, Amirkabir University of Technology (Tehran Polytechnic), Mahshahr Campus, Mahshahr, Iran*

**Abstract:** Removal of CO<sub>2</sub> in landfill gas recovery processes and fractured wells as well as its application in enhanced oil recovery and its environmental aspects are of interest. Also separation of CO<sub>2</sub> from CH<sub>4</sub> in Ethylene Oxide plant is an environmental policy of Marun Petrochemical Company. In the present work, a shell-fed hollow fiber module was modeled mathematically for CO<sub>2</sub> separation from CH<sub>4</sub>. Finite difference method was used for solving the equations. Comparison between co-current and counter-current flow patterns showed that for all conditions, counter current pattern had better efficiency for CO<sub>2</sub>/CH<sub>4</sub> separation. Influence of operating parameters such as feed pressure, permeate pressure, feed flow rate, fiber length and CO<sub>2</sub> concentration of feed on separation efficiency of CO<sub>2</sub>/CH<sub>4</sub> mixture was investigated. Also the effect of feed and permeate pressures on required membrane area showed that the membrane area increases by increasing permeate pressure and decreases by increasing feed pressure. The modeling offers valuable data about feasibility study and economical evaluation of a gas separation unit operation as a helpful unit in the industry.

**Keywords:** Hollow fiber, modeling, CO<sub>2</sub>/CH<sub>4</sub>, operating parameter, membrane area.

## 1. INTRODUCTION

The focus of much of the new awareness has turned towards examining greenhouse gas emissions and their impact on global climate [1]. Carbon dioxide which is emitted from fossil fuels, natural and refinery off-gases and many other sources is representing about 80% of greenhouse gases [2-5]. From the global environmental perspective, it is important to separate CO<sub>2</sub> from gas mixtures to avert the threat of global warming; thereby attaining the carbon emission reduction targets set out by the Kyoto Agreement [2] therefore, recovery of carbon dioxide from large emission sources is a formidable technological and scientific challenge which has received considerable attention for several years [1]. Currently, commercially available CO<sub>2</sub> separation technologies, including pressure swing adsorption, amine absorption, and cryogenic separation are highly energy intensive [6, 7], but membrane technologies are becoming more frequently used for separation of wide varying gas mixtures in different industries because of the economic competitiveness of the existing separation technologies and the present challenges of aggressive environments [8,9]. The application of membrane technology for CO<sub>2</sub> removal from CH<sub>4</sub> for upgrading the natural gas, landfill gas and enhanced oil recovery emerged in the 1980s after several major

breakthroughs [10-12]. One of the principal revolutions was the preparation of high flux asymmetric Loeb-Sourirajan membranes with selective layer thicknesses of less than 0.1µm [13]. In the last 40 years, the asymmetric single-layer hollow fiber membrane is always a favorable configuration in the membrane based gas separation systems owing to their large surface area over unit volume, self mechanical support, good flexibility and easy scale [14]. Hollow-fiber membranes are the most advantageous form of membranes used in the gas separation processes. They can be produced by any method employed for the manufacture of chemical fibers [15]. Hollow fibers are the cheapest on a per square meter basis with the highest membrane area to module volume ratio. They do not require any support, whether the feed flows inside or outside of the fiber tubes [16]. A hollow fiber module contains a large number of membrane fibers housed in a shell; its arrangement is similar to countercurrent shell and tube heat exchangers. Feed can be introduced on either the fiber or shell side, but commonly, pressurized feed gas is fed to the shell side and the components permeate at different rates to the fiber bore. Permeate is usually withdrawn in a co-current or counter-current manner, with the latter being generally more effective [17]. In co-current manner, the driving force and mass transfer rate are reduced due to concentration reduction of penetrated constituent but in counter-current mode, except of inlet and outlet sections, mass transfer rate remains constant [18]. In order to improve the performance of membrane gas separation process, optimization (operating and

\*Address corresponding to this author at the Membrane Processes Research Laboratory (MPRL), Department of Petrochemical Engineering, Amirkabir University of Technology (Tehran Polytechnic), Mahshahr Campus, Mahshahr, Iran; Tel/Fax: +98-65223-43645; E-mail: ali\_kargari@yahoo.com

design) and analysis of the process should be accomplished. Modeling and simulation are tools to achieve these objectives [19]. An appropriate modeling, offers important information about design, optimization, and the economics of membrane units. The issue of mathematical modeling of membrane gas separators was first addressed by Weller & Steiner [20]. In recent years, simulation of membrane gas separation has attracted increasing more attention and many researchers have studied modeling of hollow fiber membrane for gas separation. Boucif *et al.* [21, 22] derived an algebraic model for binary mixtures, this model was obtained from differential mass balance equations and these equations were highly non-linear. They offered numerical solution of boundary value problems encountered in hollow fiber binary gas permeators having co-current or countercurrent permeate flow with and without axial pressure drop inside the fiber bore. Chern *et al.* [23] developed a model for simulating the performance of an isothermal countercurrent hollow-fiber gas separator for binary mixture. The model equations were solved numerically as a boundary-value problem. Permeate pressure buildup has been considered explicitly and concentration dependence of the permeabilities are taken into account by using the dual-mode sorption and transport models. Rautenbach & Dahm [24] presented an analytical solution for binary mixtures in the counter current module. They considered constant permeate pressure along the permeate side. Krovvidi *et al.* [25] derived two models with different assumptions for binary mixtures in co-current and counter current module. They assumed a linear (OLM model) or quadratic (DFM model) relationship between the feed composition and the permeate composition along the membrane. The DFM model is implicit model and more accurate than OLM model (explicit model). Kovalli *et al.* [26] presented a linear approximation model (LAM) to solve the multi-component countercurrent gas permeator transport equations considering pressure variation inside the fibers. The models provided very effective and quick solution to the nonlinear coupled differential equations using the assumption of the linearity of feed and permeate side compositions. This assumption leads to algebraic analytical expressions for the prediction of membrane area and pressure ratios. Coker *et al.* [27, 28] presented a model for a multi-component gas mixture in an isothermal and non-isothermal hollow-fiber gas separation contactor that permits rapid solution of the governing differential mass and pressure distribution using a computational scheme that does not rely on conventional shooting

techniques for numerical integration. The model was developed for countercurrent, co-current and cross flow patterns with and without permeates purging. Kaldis *et al.* [29] presented a model for multi-component gas mixture; the equations were solved by orthogonal collocation to approximate differential equations, and to solve the resulting system of non-linear algebraic equations by the Brown method. Zaho *et al.* [30] simulated a binary gas separation permeator for countercurrent hollow fiber membrane modules. A differential mathematical model and an efficient numerical solution procedure based on orthogonal collocation and Quasi-Newton method was developed. Peer *et al.* [31] presented a mathematical model for simulation of gas separation in hollow fiber membrane modules with all flow patterns (cross-flow, counter-current and co-current). This model can be used for calculation of membrane performance or its required surface area for a specific separation. Madaeni *et al.* [32] modeled a counter-current module for a binary mixture. They considered as the membrane as a unit consisting of many sections and derived equations from mass balance.

Separation of CO<sub>2</sub>/CH<sub>4</sub> is the second most investigated gas pair for membrane processes. Most of the industrial processes to separate CO<sub>2</sub> from CH<sub>4</sub> are high-pressure applications with total feed pressures up to 100 bars. Depending on the fraction of CO<sub>2</sub> in these feeds, the resulting CO<sub>2</sub> partial pressures are approximately 10-50 bars [18, 33].

In this paper, separation of CO<sub>2</sub>/CH<sub>4</sub> by membrane was modeled mathematically in a hollow fiber module. Effect of operating parameters such as feed pressure; permeate pressure, feed flow rate, fiber length and CO<sub>2</sub> concentration of feed on separation efficiency of CO<sub>2</sub>/CH<sub>4</sub> mixtures of Ethylene Oxide plant of Marun Petrochemical Company was investigated. This modeling gives valuable information about feasible study optimum process and design condition and economical calculation for this separation and can be modified for separation of other gases from binary gas mixtures.

## 2. MODELING

### 2.1. Model Assumptions

The following assumptions were used for simplification of the model [31, 32]:

- 1- Module operates at steady state and isothermal conditions.

- 2- Ideal gas behavior is considered.
- 3- Mass is only transferred through selective layer and permeation mechanism is solution-diffusion.
- 4- Pressure drop in feed side is negligible.
- 5- Gas flow in both sides is plug flow.
- 6- Membrane permeability is independent of pressure and feed composition.
- 7- No axial mixing occurs due to gases flow.
- 8- All fibers have uniform outer and inner diameter and selective layer thickness is considered constant.
- 9- Fibers deformation under high pressure condition is neglected.

**2.2. Model Equations**

The permeation of gases through polymeric membrane occurs by a combination of kinetic and equilibrium controlled phenomena [17]. Diffusion of gases from selective layer can be described by Fick's first law as equation (1):

$$J_i = -D_i^* \frac{dC_i}{dl} \tag{1}$$

Where  $D_i^*$  is the concentration dependent diffusion coefficient of component  $i$  in the membrane and  $dc_i/dl$  is the concentration gradient in the permeation direction inside the membrane. Integrating Equation (1) under the assumption of constant diffusivity and connecting the concentrations at the gas/membrane and membrane/gas interfaces by Henry's law to the bulk gases properties results in Equation (2)

$$J_i = Q_i (P_F x_i - P_P y_i) \tag{2}$$

Where  $P_F$  and  $P_P$  are feed and permeate pressure side of membrane respectively, and  $Q_i$  is the permeance. Under the present assumptions, the permeability does not vary with composition and operating conditions is therefore constant.

Figure 1 shows schematic of counter current gas permeation in a hollow fiber.

The material balance for component  $i$  in a hollow-fiber module is presented as Equation (3)

$$\pm d[Lx_i] = d[Vy_i] = Q_i dA (P_F x_i - P_P y_i) \tag{3}$$

For hollow fiber:

$$dA = N_F \pi D_{LM} dz \tag{4}$$

The Hagen-Poiseuille relation [34] was used to calculate pressure drop for permeate side as Equation (5)

$$\frac{dP_P}{dz} = - \frac{128 \mu Q}{N_F \pi D_i^4} \tag{5}$$

Due to gas ideal behavior:

$$Q = \frac{T V R_g}{P_P} \tag{6}$$

By introducing the dimensionless variables as:

$$z^* = \frac{z}{l_E}; L^* = \frac{L}{F_0}; V^* = \frac{V}{F_0}; \gamma = \frac{P_P}{P_F}; \alpha_i = \frac{Q_i}{Q_n} \tag{7}$$

$$K_1 = \frac{\pi D_{LM} l_E N_F P_F P_n^G}{F_0} \tag{8}$$

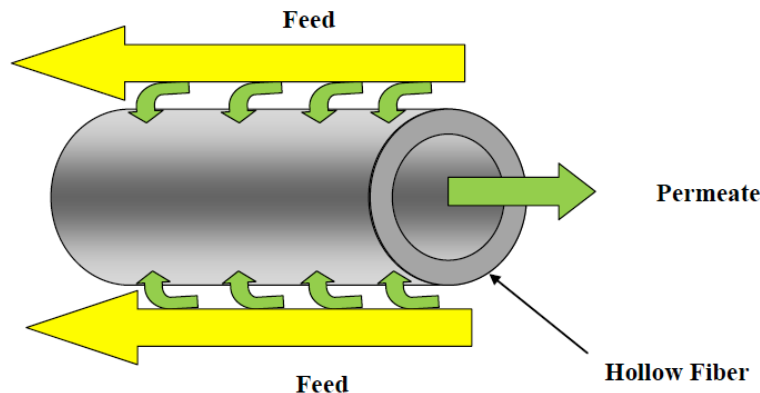


**Figure 1:** Schematic of a counter current permeation into a hollow fiber membrane.

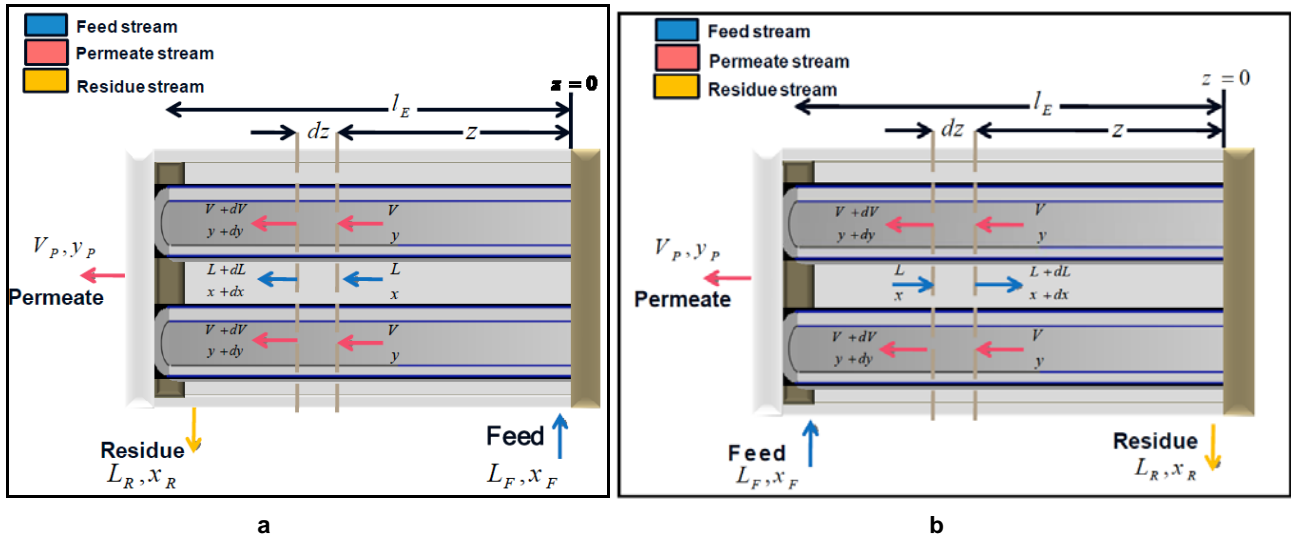


Figure 2: a, b- Co-current and countercurrent pattern in hollow fiber modules, respectively.

$$K_2 = \frac{128\mu TR_g l_E F_0}{N_F \pi D_i^4 P_F^2} \quad (9)$$

By introducing of these variables in to Equations 3 and 5, governing equations for co-current and countercurrent shell-fed hollow fiber module was obtained. Figure 2a, b present co-current and countercurrent pattern in hollow fiber modules, respectively.

Tables 1, 2 present the governing differential equations for co-current and counter-current shell-fed hollow fiber module for the present system, respectively.

Table 1: Governing Equations for Co-Current Shell-Fed Hollow Fiber Module for a Two Component System [35]

$$\frac{dx}{dz^*} = -K_1 \frac{\alpha(1-x)(x-\gamma y) - x[(1-x) - \gamma(1-y)]}{(1-V^*)} \quad (10)$$

$$\frac{dy}{dz^*} = K_1 \frac{[\alpha(1-x)(x-\gamma y) - y[(1-x) - \gamma(1-y)]]}{V^*} \quad (11)$$

$$\frac{dV^*}{dz^*} = K_1 [\alpha(x-\gamma y) + (1-x) - \gamma(1-y)] \quad (12)$$

$$\frac{d\gamma}{dz^*} = -K_2 \frac{V^*}{\gamma} \quad (13)$$

Boundary conditions: at  $z^* = 0$   $V^* = 0$ ,  $x = x_F$  and  $y = \varphi(x, \gamma)$  (14)

at  $z^* = 1$   $\gamma = \omega(\gamma_0, V^*)$  (15)

### 2.3. Solution Method

For both flow patterns, the model equations are represented by a set of coupled nonlinear boundary

value problem differential equations. Finite difference method was used [36]. Shooting method was employed for co-current pattern but for counter current flow, the resulting set of equations for  $y_i$  can be represented in matrix notation as Equation (22)

Table 2: Governing Differential Equations for Counter-Current Shell-Fed Hollow Fiber Module for a Two Component System [35]

$$\frac{dx}{dz^*} = K_1 \frac{\alpha(1-x)(x-\gamma y) - x[(1-x) - \gamma(1-y)]}{(1-V^*)} \quad (16)$$

$$\frac{dx}{dz^*} = K_1 \frac{[\alpha(1-x)(x-\gamma y) - y[(1-x) - \gamma(1-y)]]}{V^*} \quad (17)$$

$$\frac{dV^*}{dz^*} = \frac{dL^*}{dz^*} = K_1 [\alpha(x-\gamma y) + (1-x) - \gamma(1-y)] \quad (18)$$

$$\frac{d\gamma}{dz^*} = -K_2 \frac{V^*}{\gamma} \quad (19)$$

Boundary conditions: at  $z^* = 0$   $V^* = 0$  and  $y = \varphi(x, \gamma)$  (20)

at  $z^* = 1$   $L^* = 1$ ,  $x = x_F$  and  $\gamma = \omega(\gamma_0, V^*)$  (21)

$$A_i y_i = b_i \quad (22)$$

Where,  $A_i$  is the matrix of constants and the boundary conditions were appeared as boundary elements in  $b_i$  matrix. The matrix expression was written for each of the dependent variables involved in the set of differential equations. The solution of the matrix equations was started with an estimate of all the dependent variables at all the grid points. The successive iterations were proceeded till convergence achieved. Figure 3a, b show flowchart of equations

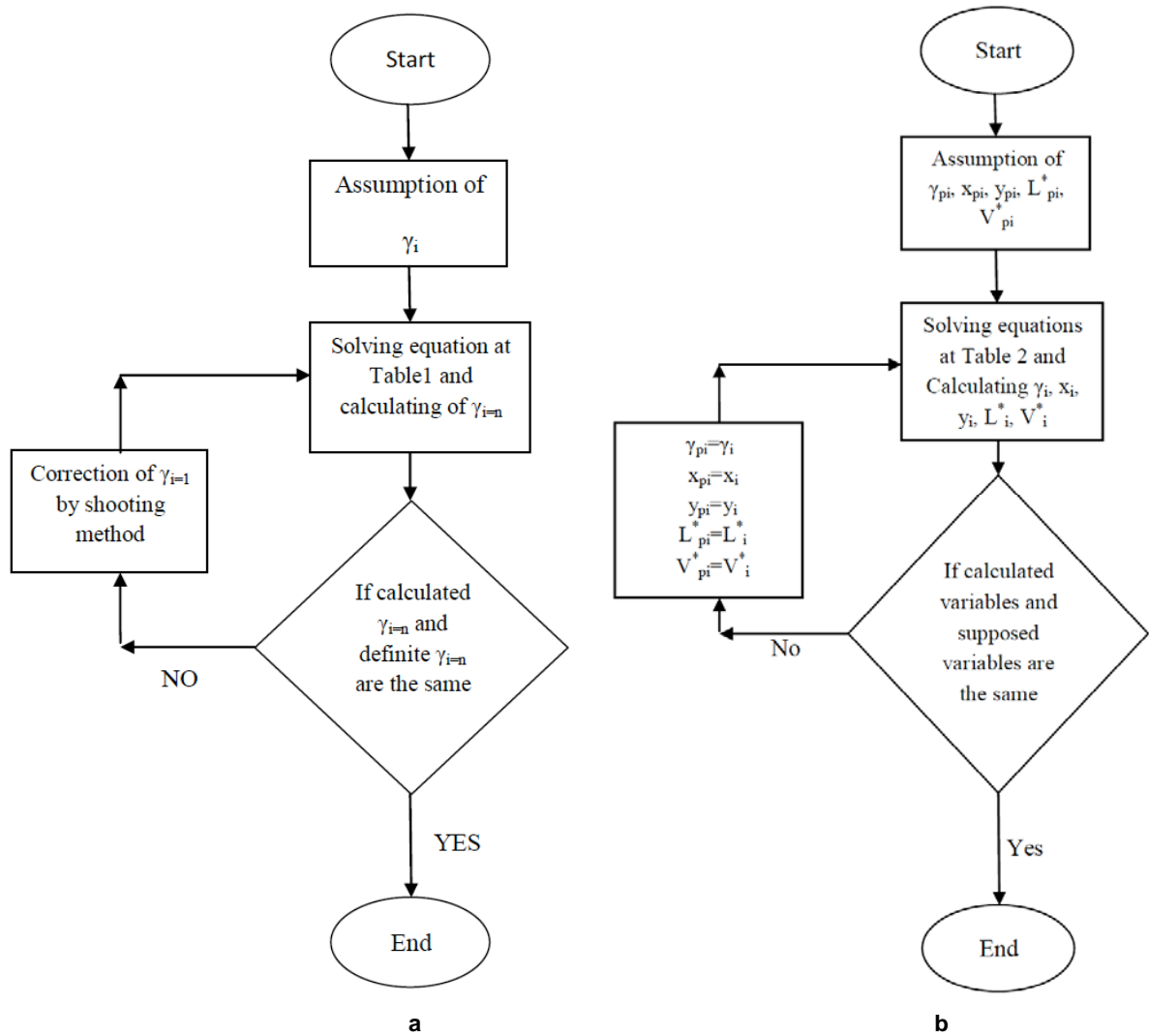


Figure 3: a, b- Flowchart of equations solution for co-current and counter-current flow pattern, respectively.

solution for co-current and counter-current flow pattern, respectively.

### 3. RESULTS AND DISCUSSIONS

The mathematical model was applied for CO<sub>2</sub>/CH<sub>4</sub> separation in a shell-fed hollow fiber module with co-current and counter-current flow patterns. The selected material for the membrane is a polyimide and the experimental values for the permeabilities are taken from Nagel *et al.* [37]. Operating conditions and module parameters have been presented in Table 3.

The concentrations of each component in permeate and retentate streams depend on design and operating conditions. Feed flow rate, feed temperature, feed and permeate pressure have been denoted to the operating condition and membrane area was considered as the design target. Feed enters in shell and permeate flows

in fibers. In fibers; CO<sub>2</sub> diffuses faster than CH<sub>4</sub> in order to higher permeability, therefore along the module CO<sub>2</sub>

Table 3: Basic Operating Conditions and Modeling Parameters for the Present Study

Parameter	Value	Unit
T	308	K
P <sub>F</sub>	35*10 <sup>5</sup>	Pa
P <sub>P</sub>	101325	Pa
Q <sub>CO2</sub>	3.207*10 <sup>-13</sup>	mol/(Pa.s.m <sup>2</sup> )
Q <sub>CH4</sub>	0.133*10 <sup>-13</sup>	mol/(Pa.s.m <sup>2</sup> )
F <sub>0</sub>	50	mol/s
l <sub>E</sub>	2	m
N <sub>F</sub>	3*10 <sup>5</sup>	-
D <sub>i</sub>	125*10 <sup>-10</sup>	m
D <sub>o</sub>	250*10 <sup>-10</sup>	m

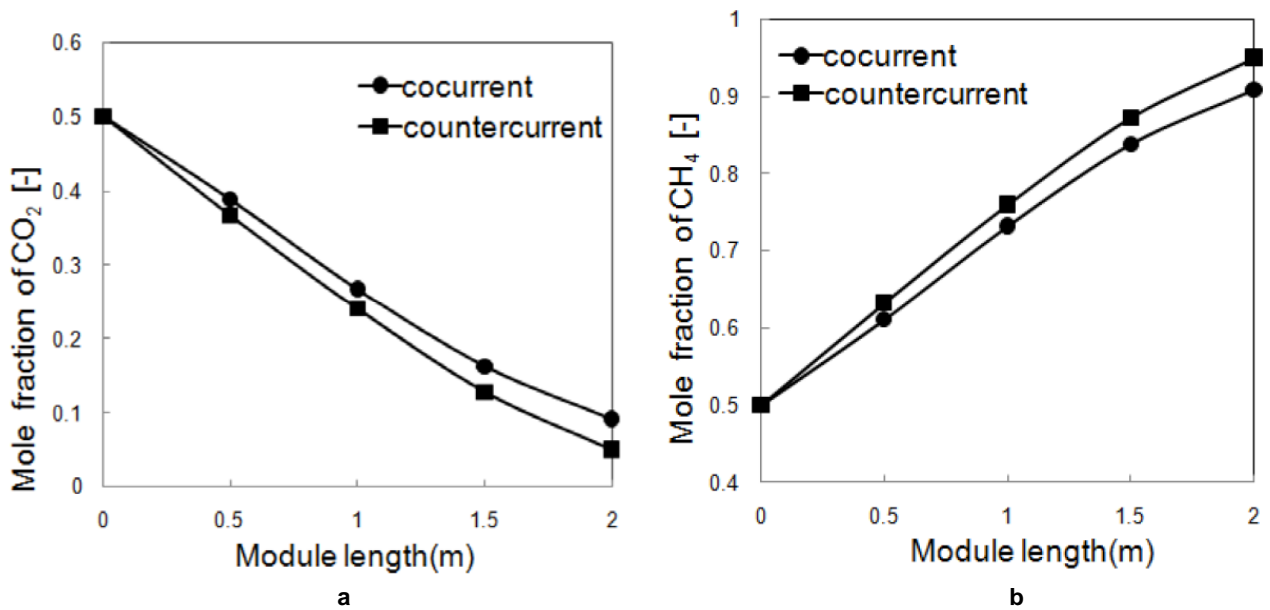


**Figure 4:** a- CO<sub>2</sub> concentration profile along the module for a (50%-50%) mixture at 35 bars and 308 K. b- CH<sub>4</sub> concentration profile along the module for a (50%-50%) mixture at 35 bars and 308 K.

concentration in shell side falls and CH<sub>4</sub> concentration increase gradually. Figures 4a, 4b show the concentration profile along the module.

### 3.1. Effect of Feed Pressure

Figure 5a represents the influence of feed pressure on CO<sub>2</sub> concentration profile in retentate stream with for co-current and counter-current flow patterns. CO<sub>2</sub> concentration decreases by increasing feed pressure

for both flow patterns but CO<sub>2</sub> concentration rate for co-current is slightly higher than counter-current. At higher feed pressure; the driving force for mass transfer increases and, therefore, the CO<sub>2</sub> purity of the permeate is enhanced. Increasing feed pressure results in more CO<sub>2</sub> passage through membrane and therefore less CO<sub>2</sub> in retentate stream.

By increasing feed pressure, CH<sub>4</sub> passage through membrane is also increased but less than CO<sub>2</sub>,

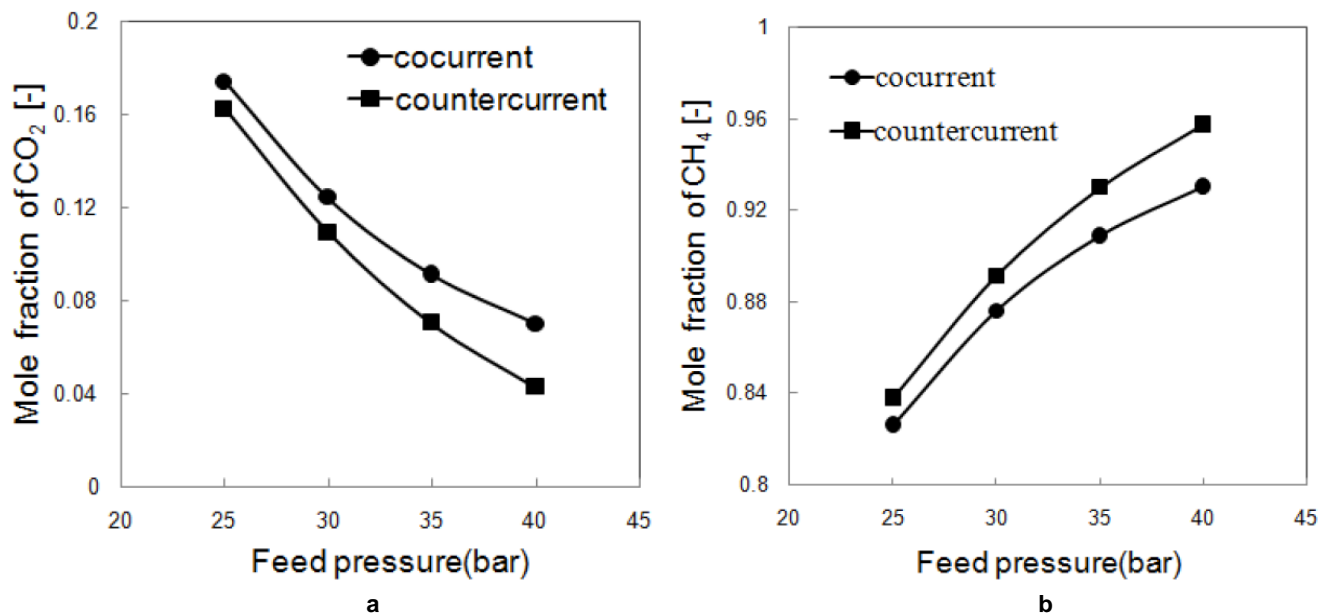


**Figure 5:** a- CO<sub>2</sub> concentration profile in retentate stream with feed pressure in co-current and counter-current flow patterns for a (50%-50%) mixture at 308 K. b- CH<sub>4</sub> concentration profile in retentate stream with feed pressure in co-current and counter-current flow patterns for a (50%-50%) mixture at 308 K.

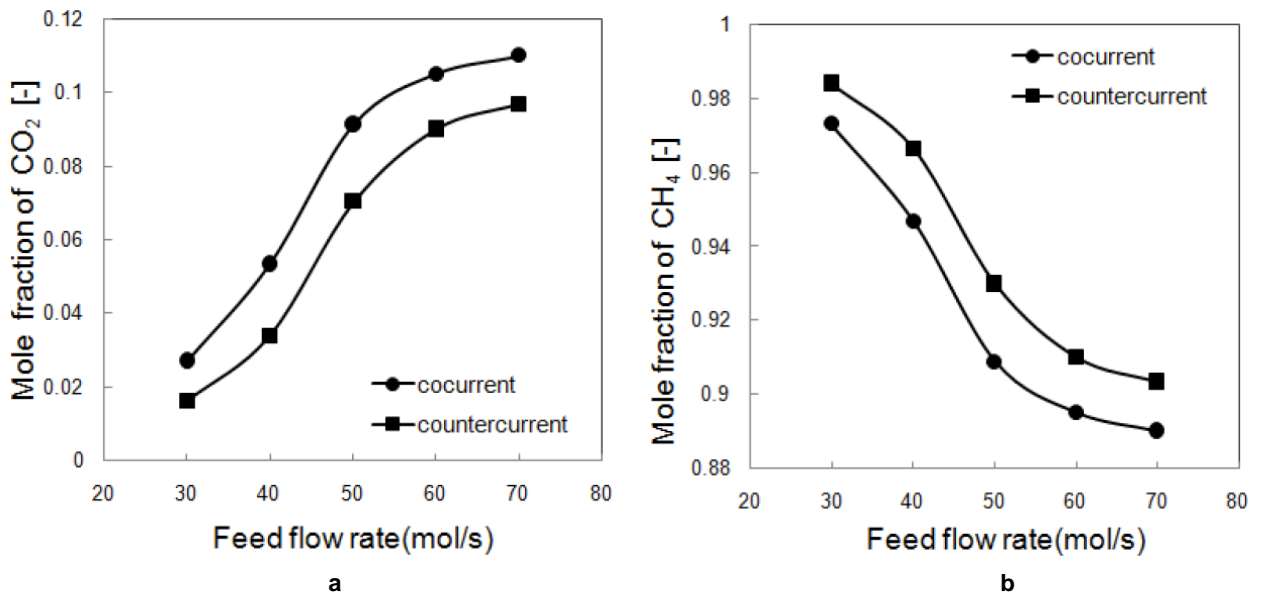


**Figure 6:** a- Influence of feed flow rate on CO<sub>2</sub> concentrations in retentate for co-current and counter-current flow patterns for a (50%-50%) mixture at 35 bars and 308 K. b- Influence of feed flow rate on CH<sub>4</sub> concentrations in retentate for co-current and counter-current flow patterns for a (50%-50%) mixture at 35 bars and 308 K.

therefore CH<sub>4</sub> concentration in retentate will be increased (Figure 5b).

### 3.2. Effect of Feed Flow Rate

The influence of feed flow rate on CO<sub>2</sub> and CH<sub>4</sub> permeation for co-current and counter-current flow patterns have been shown in Figures 6a and 6b.

By increasing feed flow, the fraction of CO<sub>2</sub> removed from the feed decreases, consistent with the

shorter contact time of the high-pressure residue gas with the active membrane area at higher feed flow rates, therefore the concentration of CO<sub>2</sub> in retentate will be increased.

### 3.3. Effect of Permeate Pressure

Permeate pressure is a key parameter for membrane unit design. The CH<sub>4</sub> and CO<sub>2</sub> concentration profile in retentate for co-current and

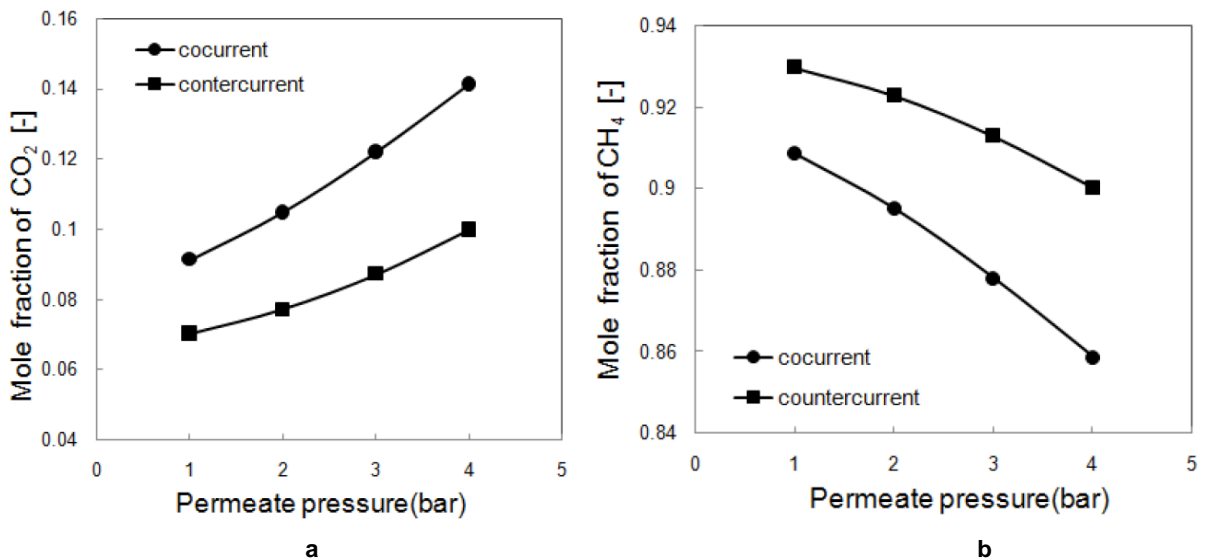


**Figure 7:** a- CO<sub>2</sub> concentration profile in retentate for co-current and counter-current flow patterns as a function of permeate pressure for a (50%-50%) mixture at 35 bars and 308 K. b- CH<sub>4</sub> concentration profile in retentate for co-current and counter-current flow patterns as a function of permeate pressure for a (50%-50%) mixture at 35 bars and 308 K.

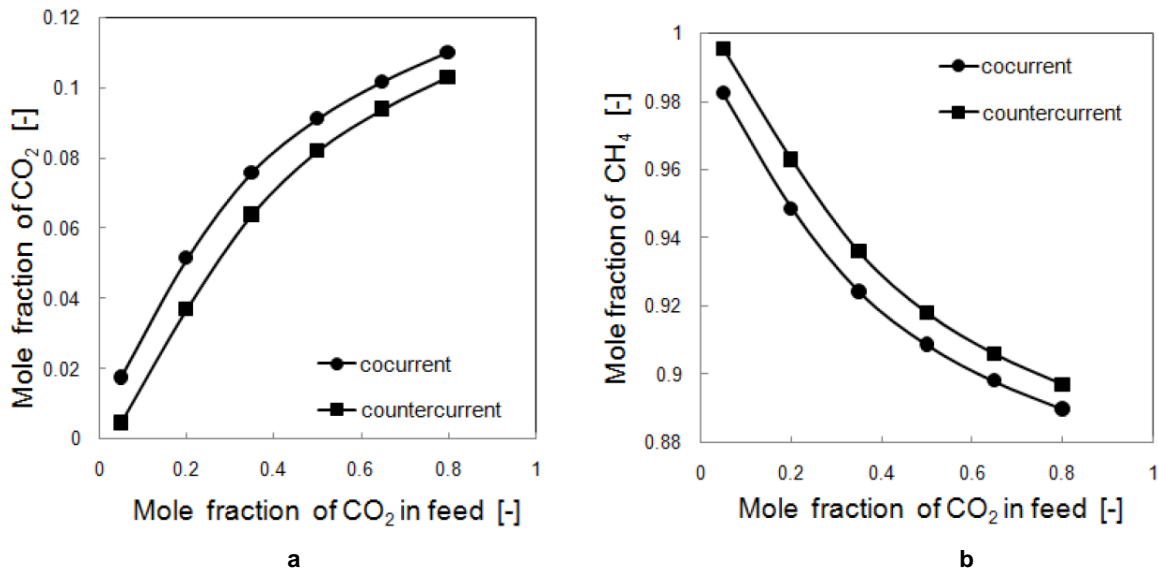


**Figure 8:** a- Influence of CO<sub>2</sub> concentration in feed on CO<sub>2</sub> concentrations in retentate for co-current and counter-current flow patterns at 35 bars and 308 K.

b- Influence of CO<sub>2</sub> concentration in feed on CH<sub>4</sub> concentrations in retentate for co-current and counter-current flow patterns at 35 bars and 308 K.

counter-current flow patterns as a function of permeate pressure have been depicted in Figures 7a and 7b.

The results showed the permeate pressure has considerable effect on CO<sub>2</sub> concentration in the retentate due to driving force reduction for both flow patterns, but the co-current pattern is more sensitive than counter-current. By increasing pressure, CO<sub>2</sub> passage through the membrane will be decreased.

Opposite behavior was observed for CH<sub>4</sub> concentration profiles in retentate stream for co-current and counter-current patterns.

### 3.4. Effect of CO<sub>2</sub> Concentration in Feed

The most important parameter in membrane process design is concentration of impurities in feed. Required membrane area and the number of modules

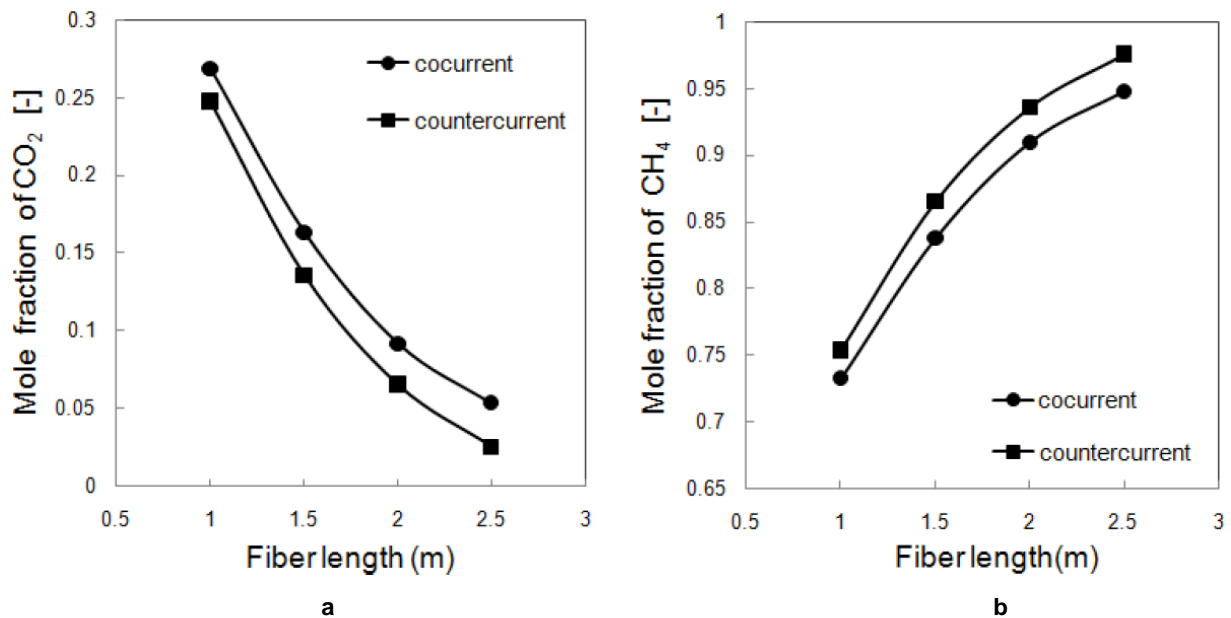


**Figure 9:** a- Effect of fiber's length on CO<sub>2</sub> concentration profiles in retentate stream for co current and counter current flow patterns for a (50%-50%) mixture at 35 bars and 308 K.

b- Effect of fiber's length on CH<sub>4</sub> concentration profiles in retentate stream for co current and counter current flow patterns for a (50%-50%) mixture at 35 bars and 308 K.

depend on the impurities in feed. In CO<sub>2</sub>/CH<sub>4</sub> separation, as feed CO<sub>2</sub> concentration increases, the amount of gas that can be diffused decreases because more CO<sub>2</sub> must be removed from the feed gas with a fixed amount of membrane area. Figures 8a, 8b represent the influence of CO<sub>2</sub> concentration in feed on CO<sub>2</sub> and CH<sub>4</sub> concentrations in retentate for both co-current and counter-current patterns, respectively.

### 3.5. Effect of Fiber's Length

By increasing fiber's length, membrane area raises. This arrangement will prepare higher membrane area and leads to higher permeation of gases. More permeation of CO<sub>2</sub> makes higher concentration of CO<sub>2</sub> compared with CH<sub>4</sub> in permeate stream, therefore by increasing fiber's length while the number of fibers are constant, CO<sub>2</sub> concentration in permeate stream will be raised. Figures 9a and 9b indicate the effect of fiber's length on CO<sub>2</sub> and CH<sub>4</sub> concentration profiles in retentate stream for co-current and counter-current flow patterns, respectively.

### 3.6. Effect of Feed and Permeate Pressures on Membrane Area

Membrane area is considered as the most important design variable for economical evaluation. Increasing membrane area can raise capital cost; therefore optimum condition should be determined. Pressure changing of feed and permeate change the membrane area for a special permeate purity. Figure 10 indicates the influence of permeate and feed pressures on

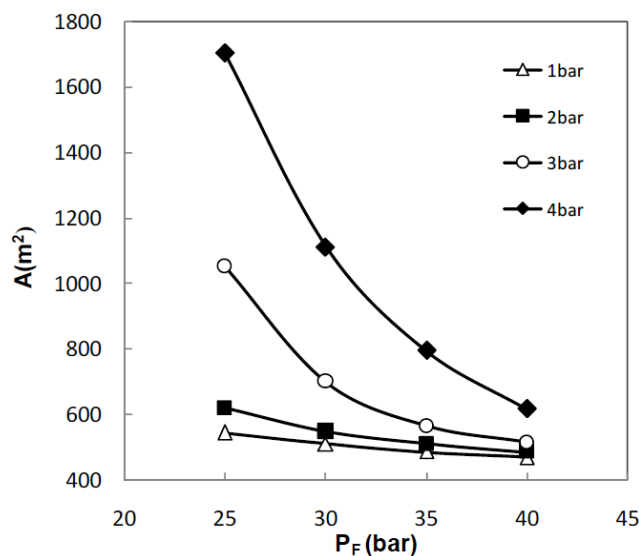


**Figure 10:** Influence of permeate and feed pressures on membrane area for 98% purity of methane in permeate stream in counter current flow pattern at 308 K.

membrane area for 98% purity of methane in permeate stream in a counter current flow pattern. Results show the required membrane area is raised by increasing permeate pressure and declined by increasing feed pressure. Also it is obvious that required membrane area increases sharply for low pressure feeds and high pressure permeates.

## 4. CONCLUSION

A shell-fed co-current and counter-current hollow fiber module was modeled mathematically for CO<sub>2</sub> separation from CH<sub>4</sub> in Ethylene Oxide plant of Marun Petrochemical Company as an environmental policy. This model is valid to predict specifications of retentate and permeate streams at various conditions. Comparison of co-current and counter-current flow patterns showed such as the other unit operations, the counter current pattern had better efficiency for CO<sub>2</sub>/CH<sub>4</sub> separation for all conditions. It was found that feed flow rate, feed pressure and module fiber length had direct effect and permeate pressure had adverse effect on CH<sub>4</sub> purity in the retentate for both flow patterns. Also required membrane area increased by increasing permeates pressure and decreased by increasing feed pressure. Because of having no data about fixed properties of used membrane and changing membrane behavior with temperature, study of these parameters on separation factor were impossible. Application of a membrane with much information about membrane properties and performance is suggested. Modeling of CO<sub>2</sub> separation from ternary and multi-component gas mixture and comparison of finite difference method with other solving methods such as orthogonal collocation are future directions of this work.

## 5. NOMENCLATURES

A = membrane area, [m<sup>2</sup>]

A<sub>i</sub> = see equation 22, [-]

b<sub>i</sub> = see equation 22, [-]

C<sub>i</sub> = concentration of component i, [mol/m<sup>3</sup>]

D<sub>i</sub><sup>\*</sup> = diffusion coefficient for component i, [m<sup>2</sup>/s]

D<sub>i</sub> = inner diameter of fiber, [m]

D<sub>LM</sub> = log mean diameter of fiber, [m]

D<sub>o</sub> = outer diameter of fiber, [m]

$F_0$  = feed flow rate, [mol/s]  
 $J_i$  = diffusion of component i, [mol/ (m<sup>2</sup>.s)]  
 $K_1$  = constant see equation 8, [-]  
 $K_2$  = constant see equation 9, [-]  
 $L^*$  = dimensionless form of retentate flow rate, [-]  
 $L$  = retentate flow rate, [mol/s]  
 $l_E$  = effective length of fiber in module, [m]  
 $N_F$  = number of fibers, [-]  
 $P_F$  = feed pressure, [Pa]  
 $P_n^G$  = Permeability of component n, [mol/ (m.Pa.s)]  
 $P_P$  = permeate pressure, [Pa]  
 $Q$  = Volumetric flow rate in permeate side, [m<sup>3</sup>/s]  
 $Q_i$  = Permeance of component i, [mol/ (m<sup>2</sup>.Pa.s)]  
 $R_g$  = Universal gas constant, [Pa.m<sup>3</sup>/ (mol.K)]  
 $T$  = Temperature, [K]  
 $V^*$  = dimensionless form of permeate flow rate, [-]  
 $V$  = permeate flow rate, [mol/s]  
 $x$  = mole fraction of fast gas in shell side, [-]  
 $x_F$  = mole fraction in feed, [-]  
 $y$  = mole fraction of fast gas in tube side, [-]  
 $z^*$  = dimensionless form of diffusion direction, [-]  
 $z$  = diffusion direction, [m]

### Greek Letters

$\alpha_i$  = selectivity for component i, [-]  
 $\gamma$  = permeate pressure to feed pressure ratio, [-]  
 $\mu$  = gas mixture viscosity, [Pa/s]  
 $\omega$  = see equation 15, 21, [-]

### REFERENCE

- [1] Yampolskii Y, Freeman BD. Membrane gas separation. John Wiley & Sons, New York 2010. <http://dx.doi.org/10.1002/9780470665626>
- [2] Sohrabi MR, Marjani A, Morad, S, Davallo M, Shirazian, S. Mathematical modeling and numerical simulation of CO<sub>2</sub> transport through hollow-fiber membranes. *Appl Math Modeling* 2011; 35: 174-88. <http://dx.doi.org/10.1016/j.apm.2010.05.016>
- [3] Al-Marzouqi MH, El-Naas MH, Marzouk SAM, et al. Modeling of CO<sub>2</sub> absorption in membrane contactors. *Sep Purif Tech* 2008; 59: 286-93. <http://dx.doi.org/10.1016/j.seppur.2007.06.020>
- [4] Khoo HH, Tan RBH. Life cycle investigation of CO<sub>2</sub> recovery and sequestration. *Environ Sci Tech* 2006; 40: 4016-24. <http://dx.doi.org/10.1021/es051882a>
- [5] Ji P, Caoa Y, Zhaoa H, et al. Preparation of hollow fiber poly (N, N-dimethylaminoethyl methacrylate)- poly (ethylene glycol methyl ether methyl acrylate)/polysulfones composite membranes for CO<sub>2</sub>/N<sub>2</sub> separation. *J Membrane Sci* 2009; 342: 190-97. <http://dx.doi.org/10.1016/j.memsci.2009.06.038>
- [6] Basu S, Cano-Odena A, Vankelecom IFJ. Asymmetric membrane based on Matrimid® and polysulphone blends for enhanced permeance and stability in binary gas (CO<sub>2</sub>/CH<sub>4</sub>) mixture separations. *Sep Purif Tech* 2010; 75: 15-21. <http://dx.doi.org/10.1016/j.seppur.2010.07.004>
- [7] Basu S, Khan A, Cano-Odena A, Liu C, Vankelecom IFJ. Membrane based technologies for biogas separations. *Chem Soci Rev* 2010; 39: 750-68. <http://dx.doi.org/10.1039/b817050a>
- [8] Takht Ravanchi M, Kaghazchi T, Kargari A. Application of membrane separation processes in petrochemical industry: a review. *Desalination* 2009; 235(1-3): 199-44. <http://dx.doi.org/10.1016/j.desal.2007.10.042>
- [9] Vu DQ, Koros WJ, Miller SJ. Mixed matrix membranes using carbon molecular sieves I. Preparation and experimental results. *J Membrane Sci* 2003; 211: 311-34. [http://dx.doi.org/10.1016/S0376-7388\(02\)00429-5](http://dx.doi.org/10.1016/S0376-7388(02)00429-5)
- [10] Sanaeepur H, Ebadi Amooghin A, Moghadassi AR, et al. CO<sub>2</sub>/CH<sub>4</sub> Separation via Polymeric Blend Membrane. *Iranian J Polym Sci Tech* 2010; 23(1): 17-28.
- [11] Ebadi Amooghin A, Sanaeepur H, Moghadassi AR, et al. Modification of ABS Membrane by PEG for Capturing Carbon Dioxide from CO<sub>2</sub>/N<sub>2</sub> Streams. *Sep Sci Tech* 2010; 45(10): 1385-94. <http://dx.doi.org/10.1080/01496391003705631>
- [12] Staudt-Bickela C, Koros WJ. Improvement of CO<sub>2</sub>/CH<sub>4</sub> separation characteristics of polyimides by chemical crosslinking. *J Membrane Sci* 1999; 155: 145-54. [http://dx.doi.org/10.1016/S0376-7388\(98\)00306-8](http://dx.doi.org/10.1016/S0376-7388(98)00306-8)
- [13] Xiao Y, Low BT, Hosseini SS, Chung TS, Paul DR. The strategies of molecular architecture and modification of polyimide-based membranes for CO<sub>2</sub> removal from natural gas—A review. *Prog Polym Sci* 2009; 34: 561-80. <http://dx.doi.org/10.1016/j.progpolymsci.2008.12.004>
- [14] Li Y, Chung TS, Xiao Y. Superior gas separation performance of dual-layer hollow fiber membranes with an ultrathin dense-selective layer. *J Membrane Sci* 2008; 325: 23-27. <http://dx.doi.org/10.1016/j.memsci.2008.08.018>
- [15] Soni V, Abildskov J, Jonsson G, Gani R. A general model for membrane-based separation processes. *Comput Chem Eng* 2009; 33: 644-59. <http://dx.doi.org/10.1016/j.compchemeng.2008.08.004>
- [16] Antonson CR, Gardner RJ, King CF, Ko DY. Analysis of gas separation by permeation in hollow fibers. *Ind Eng Chem Process Design and Development* 1977; 16(4): 463-69. <http://dx.doi.org/10.1021/i260064a005>
- [17] Tessendorf S, Gani R, Michelsen ML. Modeling, simulation and optimization of membrane-based gas separation systems. *Chem Eng Sci* 1999; 54: 943-55. [http://dx.doi.org/10.1016/S0009-2509\(98\)00313-3](http://dx.doi.org/10.1016/S0009-2509(98)00313-3)

- [18] Simons K, Nijmeijer K, Sala JG. CO<sub>2</sub> sorption and transport behavior of ODP-PA-based polyetherimide polymer films. *Polymer* 2010; 51: 3907-17. <http://dx.doi.org/10.1016/j.polymer.2010.06.031>
- [19] Shokrian M, Sadrzadeh M, Mohammadi T. C<sub>3</sub>H<sub>8</sub> separation from CH<sub>4</sub> and H<sub>2</sub> using a synthesized PDMS membrane: Experimental and neural network modeling. *J Membrane Sci* 2010; 346: 59-70. <http://dx.doi.org/10.1016/j.memsci.2009.09.015>
- [20] Weller S, Steiner WA. Engineering aspects of separation of gases: Fractional permeation through membranes. *Chem Eng Prog* 1950; 46(11): 585-90.
- [21] Boucif N, Majumdar S, Sirkar KK. Series solutions for a gas permeator with countercurrent and cocurrent flow. *Ind Eng Chem Fundamentals* 1984; 23(4): 470-80. <http://dx.doi.org/10.1021/i100016a016>
- [22] Boucif N, Sengupta A, Sirkar KK. Hollow-Fiber Gas Permeator with Countercurrent or Cocurrent Flow: Series Solution. *Ind Eng Chem Fundamentals* 1986; 25: 217-28. <http://dx.doi.org/10.1021/i100022a007>
- [23] Chern RT, Koros WJ, Fedkiw PS. Simulation of a hollow-fiber gas separator: The effects of process and design variables. *Ind Eng Chem Process Design and Development* 1985; 24: 1015-22. <http://dx.doi.org/10.1021/i200031a020>
- [24] Rautenbach R, Dahm W. Simplified Calculation of Gas-Permeation Hollow-Fiber Modules for the Separation of Binary Mixtures. *J Membrane Sci* 1986; 28: 319-27. [http://dx.doi.org/10.1016/S0376-7388\(00\)82042-6](http://dx.doi.org/10.1016/S0376-7388(00)82042-6)
- [25] Krovvidi KR, Kovvali AS, Vemury S, Khan AA. Approximate solutions for gas permeators separating binary. *J Membrane Sci* 1992; 66: 103-18. [http://dx.doi.org/10.1016/0376-7388\(92\)87001-E](http://dx.doi.org/10.1016/0376-7388(92)87001-E)
- [26] Kovvali AS, Vemury S, Admassu W. Modeling of Multi-component Countercurrent Gas Permeators. *Ind Eng Chem Res* 1994; 33: 896-903. <http://dx.doi.org/10.1021/ie00028a016>
- [27] Coker DT, Freeman BD, Fleming GK. Modeling multi component gas separation using hollow-fiber membrane contactors. *AIChE J* 1998; 44(6): 1289-302. <http://dx.doi.org/10.1002/aic.690440607>
- [28] Coker DT, Allen T, Freeman BD, Fleming GK. Non-isothermal model for gas separation hollow-fiber membranes. *AIChE J* 1999; 45(7): 1451-68. <http://dx.doi.org/10.1002/aic.690450709>
- [29] Kaldis SP, Kapantaidakis GC, Sakellaropoulos GP. Simulation of multi-component gas separation in a hollow fiber membrane by orthogonal collocation — hydrogen recovery from refinery gases. *J Membrane Sci* 2000; 173: 61-71. [http://dx.doi.org/10.1016/S0376-7388\(00\)00353-7](http://dx.doi.org/10.1016/S0376-7388(00)00353-7)
- [30] Zhao SY, Zheng HD, Wang LE. Modeling binary gas separation in hollow fiber membrane and solving by orthogonal collocation. *Frontiers on separation science and technology proceedings of the 4th International Conference, China* 2004.
- [31] Peer M, Kamali SM, Mahdiarf M, Mohammadi T. Separation of hydrogen from carbon monoxide using a hollow fiber polyimide membrane: experimental and simulation. *Chem Eng Tech* 2007; 30(10): 1418-25. <http://dx.doi.org/10.1002/ceat.200700173>
- [32] Madaeni SS, Aminnejad A, Zahedi G. A new mathematical method to study CO<sub>2</sub>-CH<sub>4</sub> separation in hollow fiber module. *Indian J Chem Tech* 2010; 17: 274-81.
- [33] Robeson LM. The upper bound revisited. *J Membrane Sci* 2008; 320: 390-400. <http://dx.doi.org/10.1016/j.memsci.2008.04.030>
- [34] Bird RB, Stewart WE, Lightfoot EN. *Transport phenomena*. John Wiley & sons, New York 2002.
- [35] Sengupta A, Sirkar KK. Analysis and design of membrane permeators for gas separation. In: *Membrane separations technology, principles and applications*, Noble RD, Stern SA, editors. Netherlands: Elsevier Science B.V., 1995; pp. 499-552. [http://dx.doi.org/10.1016/S0927-5193\(06\)80013-6](http://dx.doi.org/10.1016/S0927-5193(06)80013-6)
- [36] Hoffman JD. *Numerical methods for engineers and scientists*. CRC press Taylor Francis Group 2001.
- [37] Nagel C, Günther-Schade K, Fritsch D, Strunskus T, Faupel F. Free volume and transport properties in highly selective polymer membranes. *Macromolecules* 2002; 35(6): 2071-77. <http://dx.doi.org/10.1021/ma011028d>